AMPK/MFF Activation: Role in Mitochondrial Fission and Mitophagy in Dry Eye

Fangli Peng, Dan Jiang, Wei Xu, Yining Sun, Zhiwei Zha, Xiying Tan, Jinjie Yu, Chengjie Pan, Qinxiang Zheng, and Wei Chen

School of Ophthalmology and Optometry and Eye Hospital, Wenzhou Medical University, Wenzhou, Zhejiang, China

Correspondence: Wei Chen and Qinxiang Zheng, School of Ophthalmology and Optometry and Eye Hospital, Wenzhou Medical University, 270 Xueyuan West Road, Wenzhou, Zhejiang 325027, China; chenweimd@wmu.edu.cn, zhengqinxiang@aliyun.com.

FP and DJ contributed equally to the work presented here and should therefore be regarded as equivalent authors.

Received: July 12, 2022
Accepted: October 23, 2022
Published: November 14, 2022

Citation: Peng F, Jiang D, Xu W, et al. AMPK/MFF activation: Role in mitochondrial fission and mitophagy in dry eye. *Invest Ophthalmol Vis Sci.* 2022;63(12):18. https://doi.org/10.1167/iovs.63.12.18

Purpose. To assess the role of mitochondrial morphology and adenosine monophosphate–activated protein kinase (AMPK)/mitochondrial fission factor (MFF) in dry eye and the underlying mechanisms.

Methods. Immortalized human corneal epithelial cells (HCECs) and primary HCECs were cultured under high osmotic pressure (HOP). C57BL/6 female mice were injected subcutaneously with scopolamine. Quantitative real-time PCR was used to measure mRNA expression. Protein expression was assessed by western blot and immunofluorescence staining. Mitochondrial morphology was observed by confocal microscopy and transmission electron microscopy.

Results. First, HOP induced mitochondrial oxidative damage to HCECs, accompanied by mitochondrial fission and increased mitophagy. Then, AMPK/MFF pathway proteins were increased consequent to HOP-induced energy metabolism dysfunction. Interestingly, the AMPK pathway promoted mitochondrial fission and mitophagy by increasing the recruitment of dynamin-related protein 1 (DRP1) to the mitochondrial outer membrane in the HOP group. Moreover, AMPK knockdown attenuated mitochondrial fission and mitophagy due to HOP in HCECs. AMPK activation triggered mitochondrial fission and mitophagy. Mitochondrial fission of HCECs stressed by HOP was mediated via MFF phosphorylation. MFF knockdown reversed mitochondrial fragmentation and mitophagy in HCECs treated with HOP. Inhibition of MFF protected HCECs against oxidative damage, cell death, and inflammation in the presence of HOP. Finally, we detected mitochondrial fission and AMPK pathway activation in vivo.

Conclusions. The AMPK/MFF pathway mediates the development of dry eye by positively regulating mitochondrial fission and mitophagy. Inhibition of mitochondrial fission can alleviate oxidative damage and inflammation in dry eye and may provide experimental evidence for treating dry eye.

Keywords: dry eye, AMPK, MFF, mitochondrial fission, mitophagy

Dry eye has become an important health problem in society, affecting vision and quality of life.[1,2] The core mechanism of dry eye is tear hypertonicity,[3] which can lead to excessive production of reactive oxygen species (ROS). Excessive ROS can further promote mitochondrial damage. When mitochondria are damaged, the dynamic balance between mitochondrial fusion and fission is disrupted, with mitochondria eventually shifting to a fragmented state.[4] Mitochondrial morphology and a dynamic balance are essential for maintaining mitochondrial homeostasis; however, the morphological and dynamic features of mitochondria and the mechanisms associated with dry eye remain unclear.

Mitochondrial dynamics involve mitochondrial fission and fusion that control mitochondrial morphology.[5] Mitochondrial fragmentation or fission is a universal response to stress that affects the energy state of mitochondria and thus affects the fate of organelles.[6] Excessive fission can induce mitochondrial damage, which could hurt heart muscle,[7] the pancreas,[8] and nerve cells.[9] Damaged mitochondria must be repaired or cleared to maintain intracellular homeostasis. Mitophagy is a highly regulated multistep process that selectively degrades damaged/dysfunctional mitochondria through autophagy.[10] Mitochondrial fission is a prerequisite for mitophagy that can be facilitated by mitochondrial fragmentation.[11] Moderate autophagy can remove damaged organelles from the cell and maintain intracellular homeostasis,[12] but an excess can result in autophagic cell death.[13] Whether autophagy is beneficial to dry eye is controversial.[14,15] Furthermore, the specific mechanism of autophagy activation in dry eye remains unclear.

Mitochondrial fission is mediated mainly by dynamin-related protein 1 (DRP1), a guanosine triphosphate enzyme primarily located in the cytoplasm. DRP1 initiates fission by membrane contraction and rupture when it is recruited from the cell cytoplasm to the outer mitochondrial membrane and binds to mitochondrial fission factor (MFF).[16,17] Recent studies have indicated that MFF is phosphorylated by the activation of adenosine monophosphate–activated protein kinase (AMPK),[18,19] leading to the activation of mitochondrial fission. AMPK is an important cellular energy sensor and

regulator of metabolic homeostasis[20,21] and plays an important role in the regulation of mitochondrial morphology.[19] In response to abnormal activation of AMPK, mitochondria are fragmented or excessively divided with consequent mitochondrial dysfunction and cell damage[22–24]; however, the specific mechanism of action of the AMPK/MFF/DRP1 pathway in dry eye has not been reported.

In this study, we verified the mitochondrial oxidative damage and further explored the morphological and dynamic characteristics of mitochondria in dry eye. The mechanism of the AMPK/MFF/DRP1 signaling pathway in human corneal epithelial cells (HCECs) under high osmotic pressure (HOP) and in a dry eye mouse model was explored. In addition, the study evaluated the potential therapeutic effect of inhibition of key pathway proteins to reduce mitochondrial fission and autophagy in the outcome of dry eye, providing new ideas for treatment.

Materials and Methods

Cell Culture and Hyperosmolar Stress Model

HCECs (12-SV40 human corneal epithelial cell line, HCE-2) were purchased from the American Type Cell Collection (Manassas, VA, USA). Primary HCECs were isolated for culture according to a previous protocol.[25] The medium used for the HCECs was Dulbecco's Modified Eagle Medium/Nutrient Mixture F-12 (DMEM/F-12) + 10% fetal bovine serum (FBS) + insulin–transferrin–selenium (ITS, 5 µg/mL) + 1% penicillin–streptomycin. The supplemental hormonal epithelial medium used for the primary HCECs was DMEM/F-12 (1:1) + 5% FBS + gentamicin (50 µg/mL) + amphotericin (1.25 µg/mL) + ITS (50 µg/mL) + dimethyl sulfoxide (0.5%) + cortisol (0.5 µg/mL) + epidermal growth factor (5 ng/mL). Immortalized and primary HCECs were treated in an isotonic or hyperosmotic (312 or 500 mOsm, respectively) medium prepared as described previously[26] by adding 0 or 94 mM sodium chloride.

Reagents

The ROS detection reagent, a chloromethyl derivative of 2,7-dichlorodihydrofluorescein diacetate (CM-H_2DCFDA); MitoSOX Red Mitochondrial Superoxide Indicator (M36008); and MitoTracker Deep Red FM (M22426) were purchased from Thermo Fisher Scientific (Waltham, MA, USA). Dihydroethidium was provided by MedChemExpress (Monmouth Junction, NJ, USA), and the pCT-COX8-GFP gene lentivirus for GFP-tagged mitochondria-specific HCEC was purchased from Vigene Biosciences (Rockville, MD, USA). Anti-Fis1 (10956-1-AP), Tom20 (66777-1-Ig), and MFF antibodies (17090-1-AP) were purchased from Proteintech (Rosemont, IL, USA). The following antibodies were purchased from Cell Signaling Technology (Danvers, MA, USA): DRP1 Rabbit mAb (8570s), AMPKα Antibody (2532), and Phospho-AMPKα (Thr172) (40H9) Rabbit mAb (2535). Anti-LC3B antibody (ab51520) and Anti-SQSTM1/p62 antibody (ab91526) were purchased from Abcam (Cambridge, UK). Phospho-C2orf33 (Ser172, Ser146) Polyclonal Antibody (PA5-104614) was purchased from Thermo Fisher Scientific.

Animals and Dry Eye Model

Forty female C57BL/6 mice 6 to 8 weeks of age were purchased from Jiesjie Laboratory Animal Company (Shanghai, China). The inclusion criteria were as follows: healthy mice with no corneal leukoplakia, no ocular infections or ulcers on slit-lamp examination, and a corneal fluorescein sodium staining score < 8. All animals were treated following the ARVO Statement for the Use of Animals in Ophthalmic and Vision Research.

Mice were randomly allocated to a control or dry eye group. Control group mice were raised in a normal environment (relative humidity, 60%–80%; temperature, 21°–23°C). Mice in the dry eye group were subcutaneously injected with scopolamine (SCOP, 0.5 mg/0.2 mL; Sigma-Aldrich, St. Louis, MO, USA)[27] three times a day for 5 days and were kept in a room maintained at ≤30% humidity. Ten microliters of 5% sodium fluorescein solution were instilled into the conjunctival sacs of the mice. Approximately 1 minute later, cobalt blue light was used to evaluate and score the ocular surface under a slit lamp. The ocular surface score was derived as described in a previous study.[28]

ROS Measurement

ROS activity was measured by CM-H_2DCFDA. HCECs were seeded in 96-well black plates with a transparent bottom at a concentration of 1.5×10^4 per well. Cells were washed twice with phosphate-buffered saline (PBS) and incubated in the dark with 5-µM H_2DCFDA at 37°C for 30 minutes. The cells were then washed three times with PBS and photographed immediately with a fluorescence microscope (ZEISS, Jena, Germany).

Mitochondrial ROS Measurement

Mitochondrial ROS was measured using a MitoSOX Red probe. HCECs were grown in six-well plates. After removal of the old medium, the HCECs were washed with Hank's balanced salt solution (HBSS) and incubated in the dark with 5-µM mtSOX working solution (Dojindo Molecular Technologies, Rockville, MD, USA) at 37°C for 10 minutes. Cells were then digested with trypsin and placed on a flow cytometer (BD Accuri C6 Plus Personal Cytometer; BD Biosciences, Franklin Lakes, NJ, USA) to detect the mean fluorescence intensity of the propidium iodide channel. FlowJo was used to analyze the mean fluorescence intensity.

Cell Counting Kit-8 Assay

HCECs were seeded in 96-well plates at a concentration of 1.0×10^4 per well. Cells were washed twice with PBS and incubated for 2 hours with 100 µL 10% Cell Counting Kit-8 (CCK-8) working solution. The absorbance value at 450 nm was measured using an enzyme standard (Molecular Devices, San Jose, CA, USA).

Mitochondrial Morphology Analysis

To analyze mitochondrial morphology, HCECs were transfected with pLV-mitoGFP to trace mitochondria, fixed in 4% paraformaldehyde for 10 minutes at room temperature, and imaged under a ZEISS LSM 880 confocal microscope. Mitochondrial length was measured using ImageJ software (National Institutes of Health, Bethesda, MD, USA). For quantification of mitochondrial morphology, "fragmented" indicated that most mitochondria in the cell were spherical (no

Investigative Ophthalmology & Visual Science

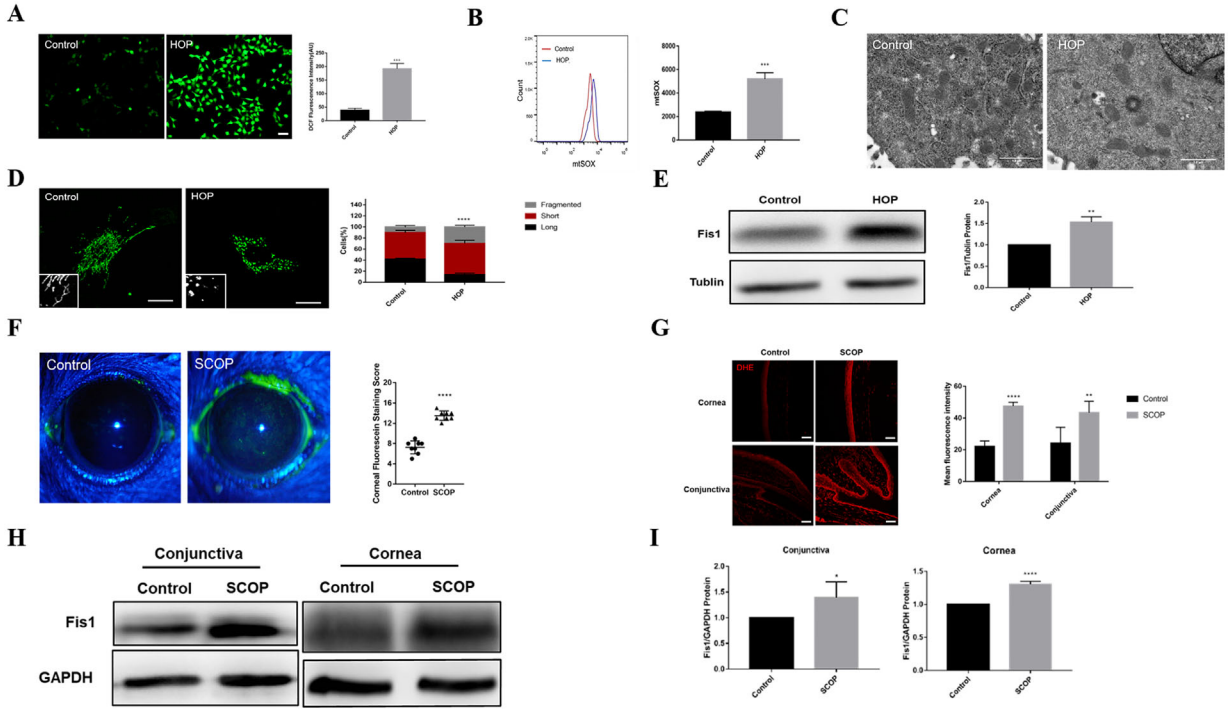

Figure 1. Hyperosmolarity induced mitochondrial oxidative damage and mitochondrial fission in vitro and in vivo. Some immortalized HCECs were treated with hyperosmotic medium and some served as controls. (**A**) H_2DCFDA fluorescence in the control and HOP groups. *Scale bar*: 50 µm. (**B**) Flow cytometry revealed the mitochondrial ROS (mtROS) level in untreated (control) and HOP-stressed HCECs. (**C**) TEM image of mitochondrial structure in HCECs after exposure to HOP or normal medium. *Scale bar*: 1 µm. (**D**) Images showing mitochondrial morphology of HCECs under the confocal microscope and quantitative analysis of fragmented mitochondria. *Scale bar*: 20 µm. (**E**) Western blot results showing the changes in Fis1 expression in untreated and HOP-stressed primary HCECs. Experimental mice were injected subcutaneously with SCOP for 5 days and placed in a dry environment. (**F**) Representative corneal staining images and mean corneal staining scores of the normal and dry eye mice. (**G**) Dihydroethidium (DHE) fluorescent staining and quantitative analysis of the corneal and conjunctival epithelium of normal and dry eye mice. *Scale bar*: 50 µm. (**H**) Western blot results showing Fis1 expression in the corneal epithelium of normal and dry eye mice. (**I**) Quantitative analysis of Fis1 protein expression. Each group had five mice. $^{*}P < 0.05$, $^{**}P < 0.01$, $^{***}P < 0.001$, $^{****}P < 0.0001$.

clear length or width), "short" indicated that most mitochondria were <10 µm, and "long" indicated most were >10 µm.[29]

Transmission Electron Microscopy Observation

HCECs were fixed in 2.5% glutaraldehyde overnight at 4°C. After fixation with osmium acid, samples were dehydrated using ethanol, permeated with acetone and epoxy resin, and then embedded with epoxy resin. Finally, the samples were sectioned and stained for observation under a transmission electron microscope (TEM, HT7700; Hitachi, Tokyo, Japan).

Real-Time PCR

An RNeasy Plus Mini Kit (QIAGEN Sciences, Inc., Germantown, MD, USA) was used to extract RNA from cells or tissues following the manufacturer's instructions. cDNA was synthesized with a cDNA synthesis kit (Takara, Beijing, China), and then gene expression was measured by real-time PCR (RT-PCR) with Applied Biosystems *Power* SYBR Green Master Mix with the 7500 Real-Time PCR System (Thermo Fisher Scientific). Relative expression of the target mRNA was normalized using glyceraldehyde-3-phosphate dehydrogenase (GAPDH) as an internal control. The sequences of the primers are shown in Supplementary Tables S1 and S2.

Western Blot Analysis

Cells and tissues were lysed in radioimmunoprecipitation assay lysis buffer. Total protein was determined using a BCA Protein Assay Kit (Beyotime, Shanghai, China). Equivalent amounts of total protein were separated by sodium dodecyl sulfate–polyacrylamide gel electrophoresis and transferred to a nitrocellulose transfer membrane (GE Healthcare Life Sciences, Chicago, IL, USA). Primary antibodies were incubated overnight at 4°C after blocking with 5% nonfat milk for 2 hours. The membranes were then incubated with horseradish peroxidase–conjugated secondary antibodies for 2 hours at room temperature. Finally, the proteins were visualized with chemiluminescence reagents (Beyotime, China). The films were scanned using a GE Amersham Imager AI680 (GE Healthcare Life Sciences).

Immunofluorescent Staining

HCECs cultured on 24-well plates were fixed in 4% paraformaldehyde for 15 minutes. Then, at room temperature, the samples were permeabilized for 15 minutes with 0.4% Triton X-100. Nonspecific binding of the samples was blocked by 20% goat serum and the samples were incubated at 4°C overnight with the primary antibodies. Secondary antibodies conjugated with Alexa Fluor 488 and 594 were incubated at room temperature in the dark for 1 hour, and

Investigative Ophthalmology & Visual Science

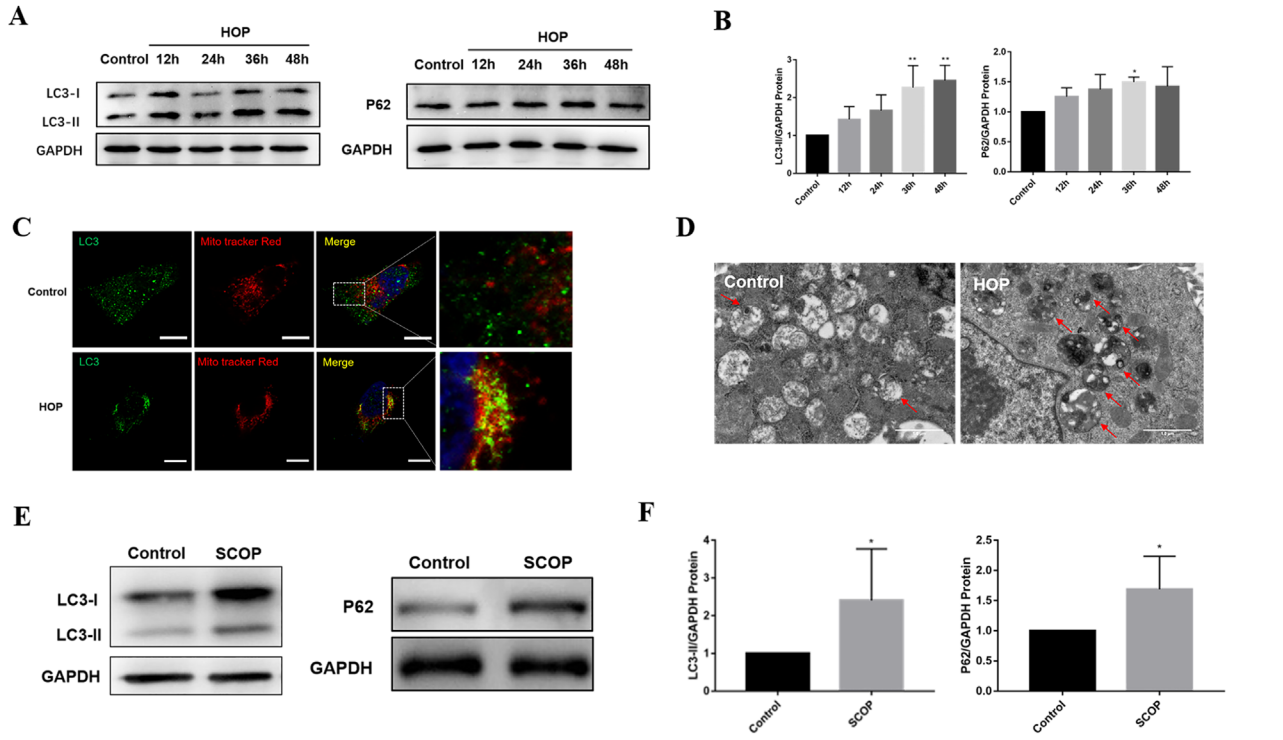

Figure 2. Excessive autophagy and mitophagy in dry eye both in vitro and in vivo. (**A**) Protein expression level of LC3 and P62 in HCECs was detected by western blot after exposure to HOP for the indicated times. (**B**) Quantitative analysis of LC3 and P62 protein expression in HCECs ($n = 3$). (**C**) Immunofluorescence images showing the co-localization of LC3 and MitoTracker Deep Red–labeled mitochondria. *Scale bar*: 20 µm. (**D**) TEM results of untreated and HOP-stressed HCECs. *Red arrows* indicate undegraded autophagolysosomes. *Scale bar*: 1 µm. (**E**) Western blot results of LC3 and P62 expression by conjunctival tissue in normal and dry eye mice. (**F**) Quantification of LC3 and P62 protein expression in dry eye mice ($n = 5$). Results are presented as mean ± SD. $^{*}P < 0.05$, $^{**}P < 0.01$.

the nuclei were stained with 4′,6-diamidino-2-phenylindole (DAPI). Finally, confocal microscopy (ZEISS LSM 800) was used to photograph the stained samples.

RNA Interference

At 50% confluence, HCECs were transfected using Invitrogen Lipofectamine RNAiMAX Transfection Reagant (Thermo Fisher Scientific) with small interfering RNA (siRNA)-targeting AMPK (forward, 5′-CUGCUGAUGCCUAGCCAGUUGGUAA-3′). Stealth siRNA was used as a negative control treatment. To reach a final concentration of 50 nM, dried siRNA was dissolved in nuclease-free water in accordance with the manufacturer's instructions.

Virus Transfection Assay

HCECs were knocked down by short hairpin RNA (shRNA)–MFF viruses or blank vectors supplied by Just Science Company (Shanghai, China), and the transduction was conducted following the manufacturer's instructions.

Statistical Analysis

All statistical analyses were carried out using GraphPad software (La Jolla, CA, USA), and results are expressed as mean ± SD. Differences between the two groups were compared using Student's *t*-test. One-way ANOVA was performed to make comparisons among three or more groups. $P < 0.05$ was considered statistically significant.

Results

Mitochondrial Oxidative Damage and Mitochondrial Fission Increased in Dry Eye

Mitochondrial oxidative damage and morphological changes were identified in HCECs in vitro. Figure 1A shows a significant increase in intracellular ROS in HOP-stressed HCECs compared with the control group and a significant increase in mitochondrial ROS production (Fig. 1B). Oxidative stress led to increased apoptosis, and HOP resulted in increased apoptosis and decreased cell viability (Supplementary Fig. S1). Compared with the control group, the expression of inflammatory factors such as NLRP3 and TNF-α was significantly enhanced in HCECs under HOP (Supplementary Fig. S2). The TEM results showed that the mitochondria were rod shaped and had a clear cristae structure in the control group, whereas those in HOP-stimulated cells were shortened with disorganized or absent cristae (Fig. 1C). Mitochondrial morphological results revealed that, in the control group, approximately 41.5% of cells had long mitochondria and 10.2% had fragmented mitochondria. Nonetheless the percentage of fragmented mitochondrial cells was significantly increased (29.8%) in the HOP group ($P < 0.0001$, $n = 3$) (Fig. 1D). In particular, fission protein 1 (Fis1) expression increased in HOP-treated primary HCECs compared with the control group, suggesting an increase

Investigative Ophthalmology & Visual Science

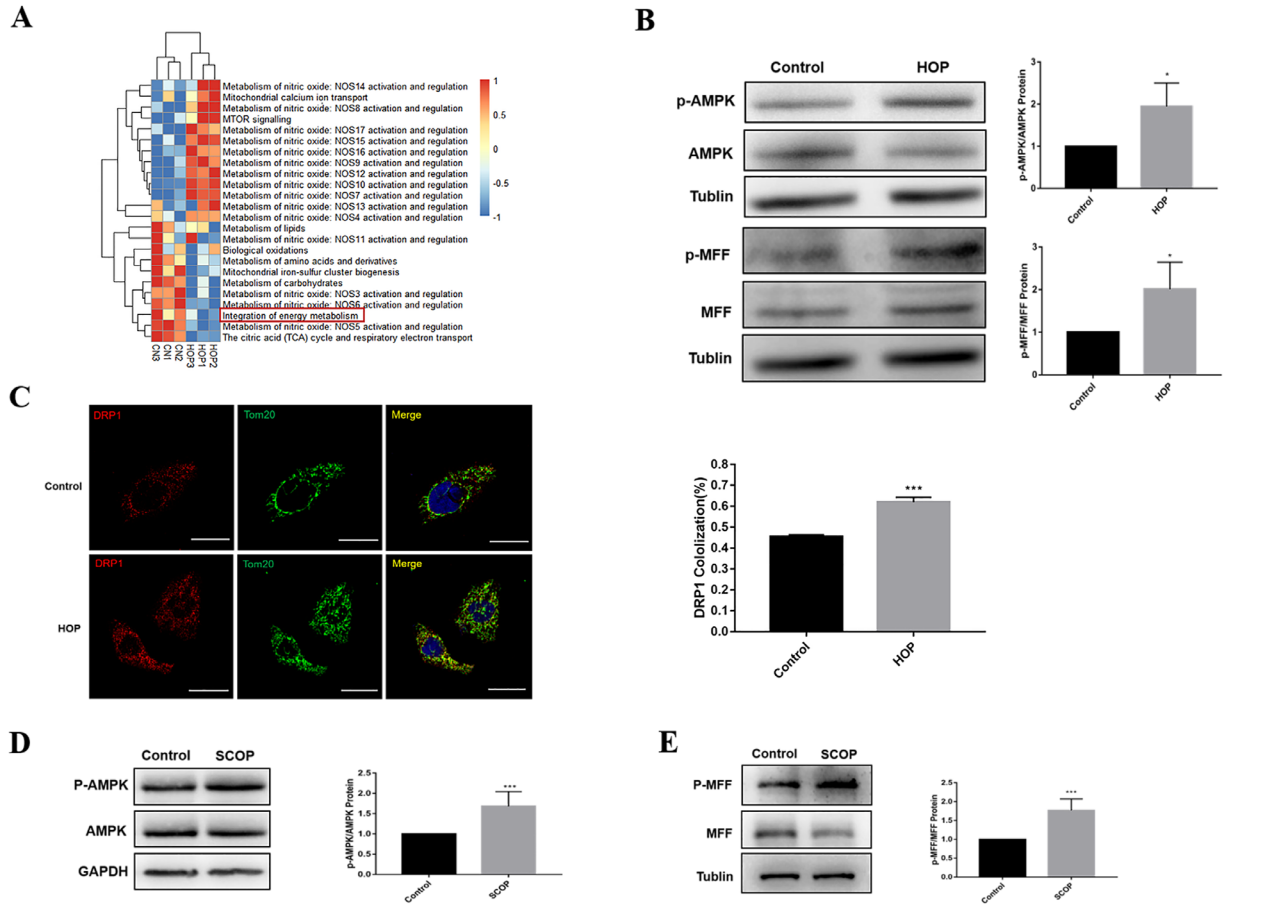

Figure 3. The AMPK/MFF/DRP1 pathway was activated in vitro and in vivo. (**A**) The differentially expressed gene sets between the control and HOP groups. (**B**) Western blot results showing the changes in AMPK, p-AMPK, MFF, and p-MFF expression after 36 hours in HCECs exposed to hyperosmotic medium relative to that in normal medium. (**C**) Immunofluorescence analysis of DRP1 and Tom20 co-localization in HCECs after HOP for 36 hours. *Scale bar*: 20 µm. Cellular results are presented as the mean ± SD of three independent experiments. (**D**) Western blot results showing AMPK and p-AMPK expression of the conjunctiva in normal and dry eye mice. (**E**) Western blot was conducted to detect MFF and p-MFF expression of the conjunctiva in normal and dry eye mice, five mice in each group. $^{*}P < 0.05$,$^{**}P < 0.01$, $^{***}P < 0.001$.

in mitochondrial fission in primary HCECs induced by HOP (Fig. 1E). These results suggest that mitochondrial homeostasis in HCECs is disrupted and is in a state of "excessive" fission.

In vivo, C57/B6 female mice were subcutaneously injected with SCOP for 5 days. Mice in the SCOP group had more obvious epithelial defects and higher ocular surface scores than mice in the normal group (Fig. 1F). Figure 1G demonstrates that, in the SCOP group, the ROS level in corneal and conjunctival epithelial cells was substantially higher than in the control group. Furthermore, Fis1 expression was significantly increased in the corneas and conjunctivas of SCOP mice (Figs. 1H, 1I). The oxidative damage and mitochondrial fission were also evident in the ocular surface epithelium of the dry eye mice.

Autophagy and Mitophagy Are Overactivated in Dry Eye

After clarifying the upregulation of mitochondrial fragmentation in dry eye, our results showed that autophagy-related gene expression increased in HOP-stressed HCECs and dry eye mice (Supplementary Figs. S3A, S3B). Figures 2A and 2B illustrate a significant increase in LC3B and P62 expression following HOP treatment. To further assess autophagy induction and autophagic flux, we treated HCECs with the autophagy inducer rapamycin and the lysosomal degradation inhibitor bafilomycin A1. As with the autophagy inducer rapamycin, HOP induced increased expression of LC3-II protein (Supplementary Fig. S4A). In the case of bafilomycin A1 treatment, HCECs subjected to HOP showed a higher LC3-II level than cells treated with only bafilomycin A1 or HOP, indicating an increase in autophagy induction and autophagic flux (Supplementary Fig. S4B). In addition, HOP increased the co-localization of LC3B with MitoTracker Deep Red, suggesting increased mitophagy in HCECs following HOP (Fig. 2C). There were more undegraded autophagosomes or autophagic lysosomes in HCECs under HOP compared with the control group (Fig. 2D), suggesting an overproduction of autophagy. Accordingly, LC3 and P62 protein expression in conjunctivas increased in dry eye mice (Figs. 2E, 2F). These data suggest that autophagy or mitophagy is overactivated in dry eye, leading to the accumulation of damaged organelles within the cell.

Investigative Ophthalmology & Visual Science

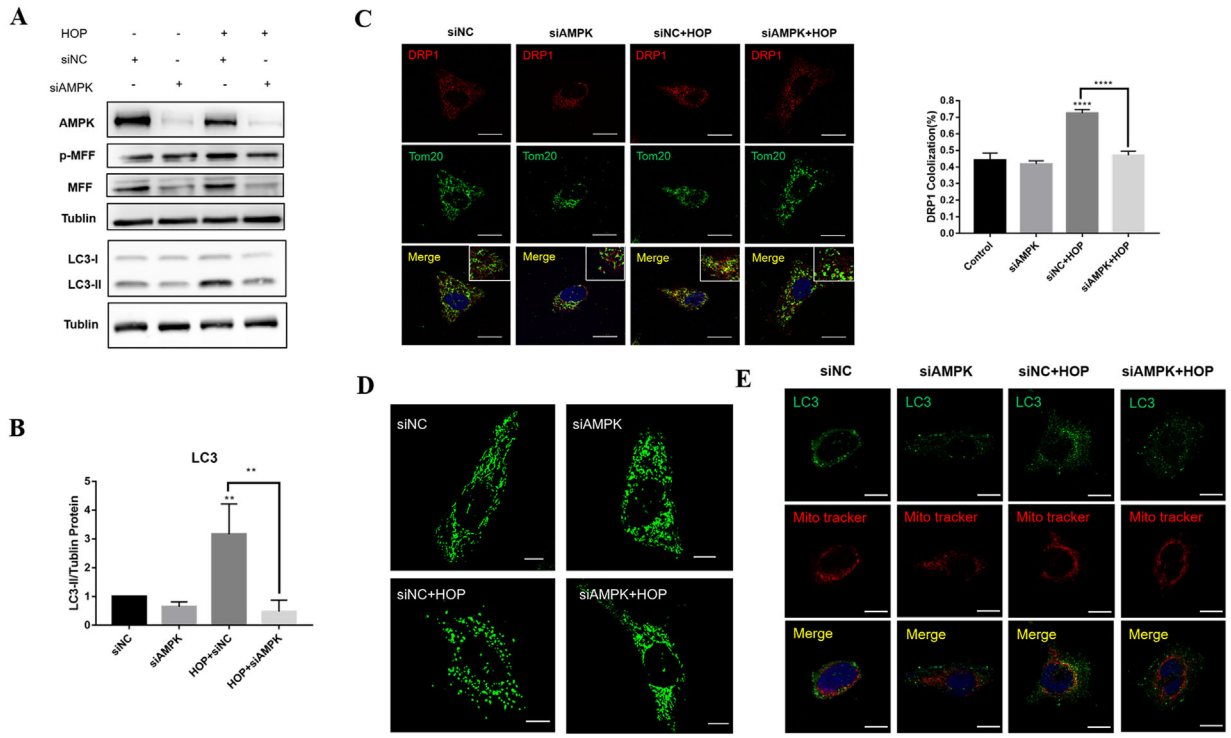

Figure 4. AMPK knockdown alleviated HOP-induced mitochondrial fission and mitophagy. (**A**) Protein expression of AMPK, p-MFF, and LC3 in transfected siAMPK and siNC cells with or without exposure to HOP. (**B**) Quantitative analysis of LC3 protein expression in HCECs. (**C**) Immunofluorescence analysis of DRP1 and Tom20 co-localization after AMPK knockdown. *Scale bar*: 20 µm. (**D**) Mitochondrial morphology of HCECs under a confocal microscope after AMPK knockdown. *Scale bar*: 10 µm. (**E**) Immunofluorescence images showing the co-localization of LC3B and MitoTracker Deep Red. *Scale bar*: 20 µm. Results are presented as mean ± SD from three independent experiments. $^{**}P < 0.01$, $^{****}P < 0.0001$.

The AMPK/MFF/DRP1 Pathway Is Activated in Dry Eye

To further understand the mechanism of mitochondrial changes in hyperosmolarity, single-sample gene set enrichment analysis (ssGSEA) was performed in R 4.1.0 (R Foundation for Statistical Computing, Vienna, Austria), using the metabolic-related pathways from the Reactome database (https://reactome.org/). The 24 pathways with the most significant changes ($P < 0.05$) are shown in Figure 3A and include downregulation of the integration of energy metabolism. The result implies that hyperosmolarity induces impaired energy metabolism in HCECs. The central metabolic sensor AMPK is activated when cells undergo energy stress.[30] In addition, HOP increased AMPK phosphorylation and the downstream substrate MFF in HCECs following exposure to HOP for 36 and 48 hours (Supplementary Fig. S5). Figure 3B shows that AMPK/MFF was also activated in primary HCECs after exposure to HOP for 36 hours. The results showed that the co-localization of DRP1 with Tom20 increased following exposure to HOP (Fig. 3C), indicating that activated MFF recruited more DRP1 to mitochondria. Therefore, HOP induced impaired energy metabolism in HCECs and activated AMPK/MFF, which recruited DRP1 from the cytoplasm to the mitochondrial outer membrane. Moreover, in vivo, AMPK/MFF expression increased significantly in the conjunctivas of dry eye mice compared with normal mice (Figs. 3D, 3E).

AMPK Participates Directly in MFF/DRP1 Signaling and Mitophagy in HCECs Under Conditions of Hyperosmolarity

Whether MFF was an AMPK-dependent substrate in HCECs under conditions of hyperosmolarity was further determined. After being transfected with siAMPK (Supplementary Fig. S6), HCECs were exposed to hyperosmotic or normal medium for 36 hours. Importantly, AMPK knockdown significantly decreased the level of MFF and its phosphorylation due to HOP (Fig. 4A). Moreover, knockdown of AMPK significantly reduced DRP1 in the mitochondrial outer membrane (Fig. 4C) and mitochondrial fragmentation in HCECs under HOP (Fig. 4D). AMPK knockdown somewhat attenuated the level of LC3 protein (Figs. 4A, 4B) and LC3 co-localization in the mitochondria (Fig. 4E). Furthermore, the AMPK activator 5-aminoimidazole-4-carboxamide ribonucleotide (AICAR) was used to upregulate AMPK and detect the changes in downstream factors. The results showed that AMPK activation in HCECs increased the phosphorylation of MFF (Fig. 5A), promoted transfer of cytoplasmic DRP1 to the outer mitochondrial membrane (Figs. 5C, 5D), and further increased mitochondrial fragmentation (Fig. 5E). Activation of AMPK increased LC3 protein expression (Figs. 5A, 5B) and LC3 co-localization on mitochondria (Fig. 5F). Overall, these results indicate that AMPK/MFF positively regulated mitochondrial fission and mitophagy by recruiting cytoplasmic DRP1 to mitochondria in HCECs.

Investigative Ophthalmology & Visual Science

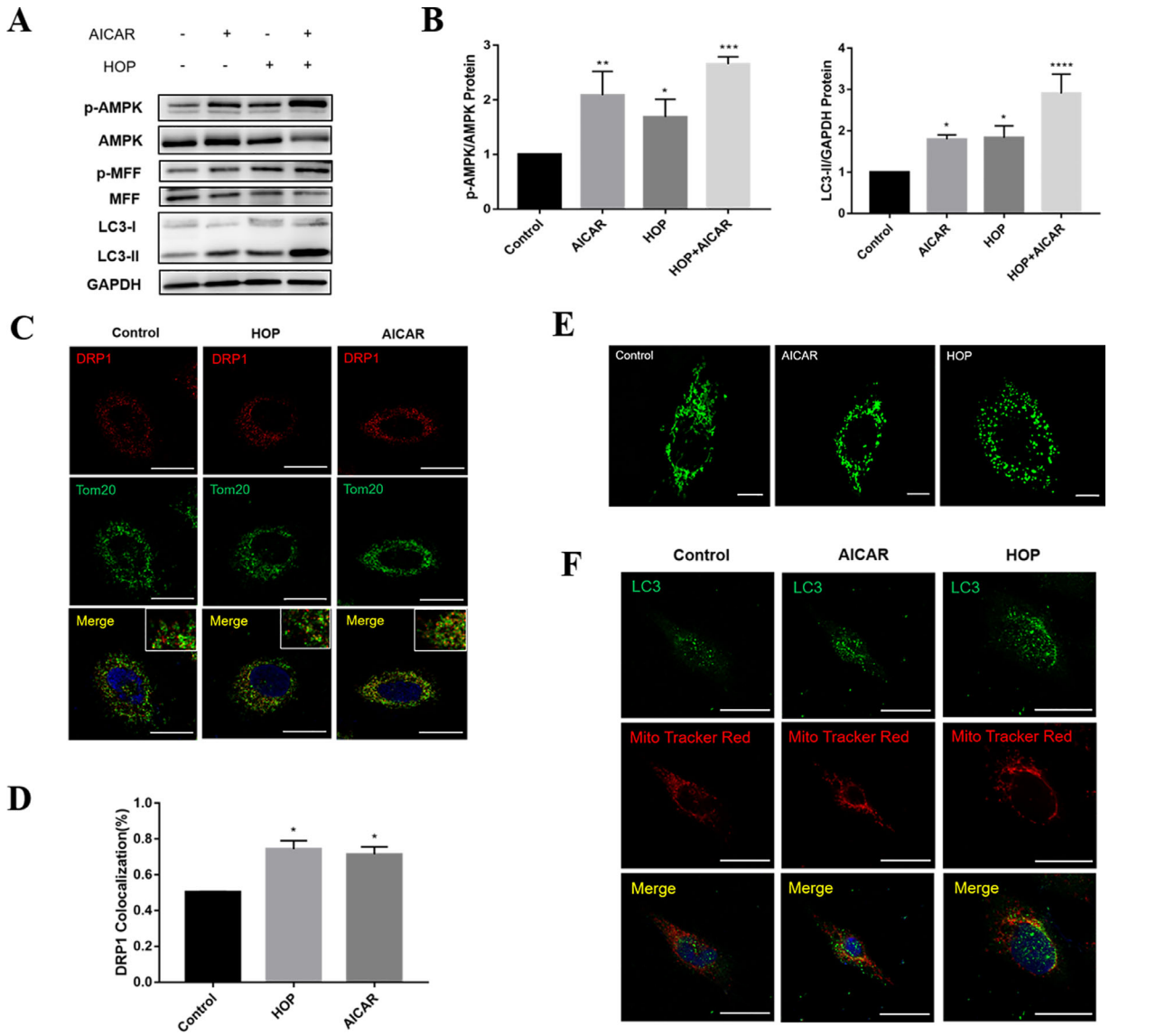

Figure 5. Activation of AMPK increased mitochondrial fission and mitophagy in HCECs. (**A**) Western blot results detected the changes in AMPK, p-AMPK, MFF, p-MFF, and LC3 expression in untreated and HOP-stressed HCECs with or without AICAR treatment. (**B**) Quantitative analysis of p-AMPK and LC3 expression after AICAR treatment. (**C**) Immunofluorescence co-localization analysis of DRP1 and Tom20 in HCECs after AICAR treatment. *Scale bar*: 20 µm. (**D**) Quantitative analysis of DRP1 co-localization with Tom20 in HCECs following AICAR treatment. (**E**) Images showing the mitochondrial morphology of HCECs under a confocal microscope after AICAR treatment. *Scale bar*: 10 µm. (**F**) Immunofluorescence images of LC3 localized on mitochondria in HCECs after AICAR treatment. *Scale bar*: 20 µm. Results are presented as mean ± SD of three independent experiments. $^{*}P < 0.05$, $^{**}P < 0.01$, $^{***}P < 0.001$, $^{***}P < 0.0001$.

MFF Is Essential in Mitochondrial Fission and Mitophagy

To verify whether MFF is a crucial factor in the regulation of mitochondrial fission and mitophagy, HCECs were transfected with blank or MFF-specific shRNA lentiviral vectors to construct a stable transfer cell line. Importantly, MFF knockdown significantly reduced DRP1 recruitment from the cytoplasm to the mitochondrial outer membrane under HOP (Figs. 6D, 6E). In addition, knockdown of MFF depressed LC3 protein expression (Figs. 6A, 6C), and LC3B localized on mitochondria under HOP (Fig. 6F). These results suggest that MFF plays a critical role in mitochondrial fission and mitophagy regulation by HOP.

Inhibition of Mitochondrial Fission Alleviates Dry Eye

To examine the possible impact of mitochondrial fission inhibition on cell fate under hyperosmolar conditions, we assessed cellular oxidative damage, cell viability, and inflammation in HCECs following shMFF knockdown. MFF knockdown reduced HOP-induced intracellular ROS levels (Figs. 7A, 7B). In addition, MFF knockdown preserved cell viability in HCECs exposed to HOP (Fig. 7C). Figure 7D shows that MFF knockdown reduced expression of NLRP3 and TNF-α at the gene level in HCECs under HOP. Therefore, the inhibition of mitochondrial fission with MFF knockdown partially alleviated dry eye.

Investigative Ophthalmology & Visual Science

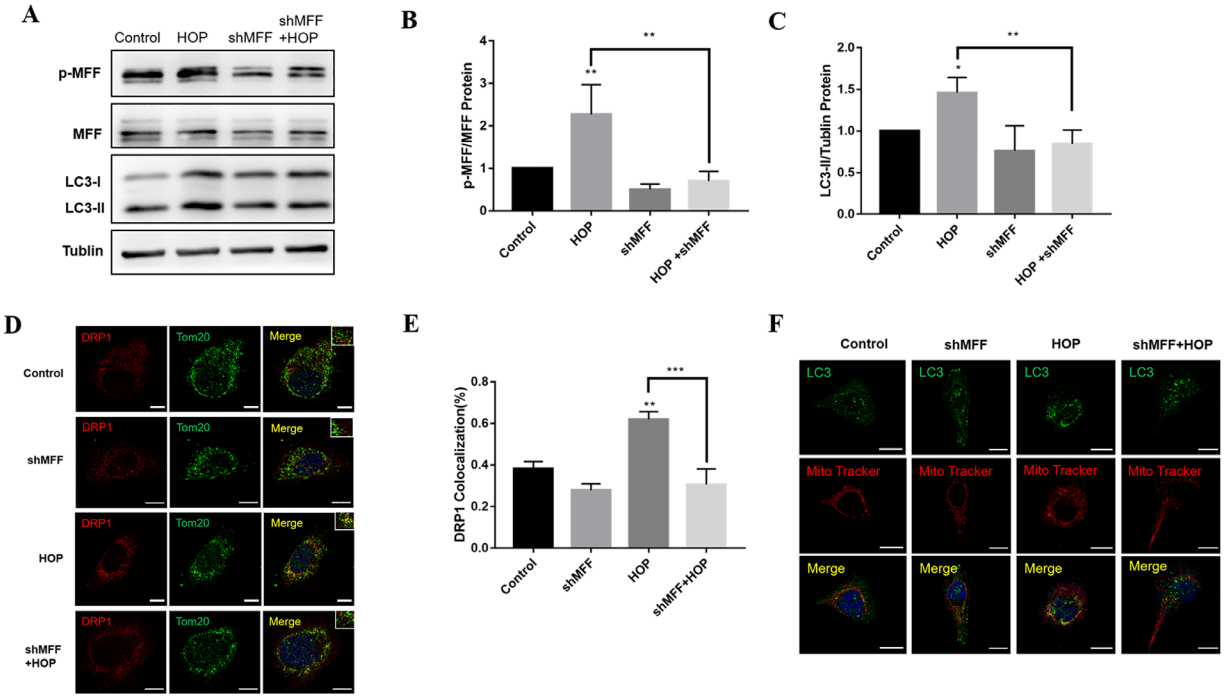

Figure 6. Knockdown of MFF alleviated HOP-induced mitochondrial fragmentation and mitophagy. Immortalized HCECs were transfected with MFF-specific shRNA or blank lentiviral vectors. The stably transfected HCECs were exposed to normal or hyperosmotic medium for 36 hours. (**A**) Western blot results of p-MFF, MFF, and LC3 expression in shMFF knockdown HCECs with or without HOP treatment. (**B**, **C**) Quantitative analysis of p-MFF and LC3 expression in HCECs following shMFF knockdown. (**D**) Immunofluorescence co-localization analysis of DRP1 and Tom20 in HCECs following shMFF knockdown. *Scale bar*: 10 µm. (**E**) Quantitative analysis of DRP1 co-localization with Tom20 in HCECs after shMFF knockdown. (**F**) Immunofluorescence images of LC3 localized on mitochondria in HCECs after shMFF knockdown. *Scale bar*: 10 µm. Results are presented as the mean ± SD of three independent experiments. $^{**}P < 0.01$,$^{***}P < 0.001$.

Therefore, in dry eye, AMPK/MFF regulates intracellular mitochondrial fission and mitophagy by recruiting DRP1 from the cytoplasm to the outer mitochondrial membrane in HCECs (Fig. 8).

Discussion

Our study determined that HOP leads to extensive mitochondrial fission and mitophagy in HCECs. AMPK is activated in HCECs as a result of disturbed energy metabolism under HOP. Moreover, AMPK activation phosphorylates MFF, which recruits DRP1 to the mitochondrial outer membrane and mediates mitochondrial fission and mitophagy. Inhibition of mitochondrial fission by inhibiting MFF reverses the return of dry eye. Therefore, mitochondrial fission is closely related to dry eye, and excessive mitochondrial fission and mitophagy regulated by the AMPK/MFF/DRP1 pathway are likely to play a key role in the pathogenesis of dry eye.

Mitochondrial morphology is closely related to function, including the generation of ROS, synthesis of adenosine triphosphate, and regulation of apoptosis.[31] The shape of the mitochondria is a result of a balance of fusion and fission to meet metabolic demands and remove damaged mitochondria.[32] Cellular dysfunction causes mitochondrial fission and has been observed in neuromuscular[33] and cardiovascular diseases,[34] as well as cancer.[35] Yu et al.[36] suggested that dynamic changes to mitochondrial morphology are a necessary causal factor in the increase of ROS induced by high glucose. Interestingly, we found that HOP induced mitochondrial fission in dry eye. In addition, our study detected an abnormal increase in autophagy and mitophagy in dry eye. Mitochondrial fission or fragmentation contributes to the autophagic clearance of mitochondria, also referred to as mitophagy.[37] Abnormal activation of autophagy is thought to lead to apoptosis of HCECs in dry eye.[14] Our results suggest that excessive mitophagy due to increased mitochondrial fission may be the pathological mechanism of dry eye.

AMPK is a key cellular energy sensor and regulator of metabolic homeostasis, and several studies have reported that MFF is an AMPK-dependent substrate.[18,20] The cytoplasmic structural domain in MFF recruits DRP1 to the mitochondrial splitting site, allowing DRP1 oligomers to constrict and segment the mitochondrial membrane.[38] Submitochondrial localization of DRP1 promotes mitochondrial fission.[39] Importantly, we found that AMPK phosphorylation activated MFF that recruited DRP1 to translocate from the cytoplasm to the outer mitochondrial membrane in HCECs after exposure to HOP. Therefore, the results suggest that AMPK/MFF activation is involved in mitochondrial fission in dry eye. By up- and downregulating AMPK expression, AMPK positively regulated downstream MFF/DRP1 to mediate mitochondrial fission and mitophagy. Nonetheless, MFF knockdown in HOP-stressed HCECs resulted in reduced recruitment of DRP1 to the mitochondrial outer membrane and reduced mitophagy compared with that in the HOP group. Our data suggest that the AMPK/MFF/DRP1 pathway plays a crucial role in promoting HOP-induced mitochondrial fission and mitophagy in HCECs.

By inhibiting DRP1, excessive apoptosis and mitochondrial integrity are reversed in cell models of Cockayne syndrome group A.[40] When MFF was knocked down in HS-27a cells, iron overload–induced mitochondrial fragmentation was fully diminished, cell apoptosis was reduced, and cell viability was increased, accompanied by weakened

Investigative Ophthalmology & Visual Science

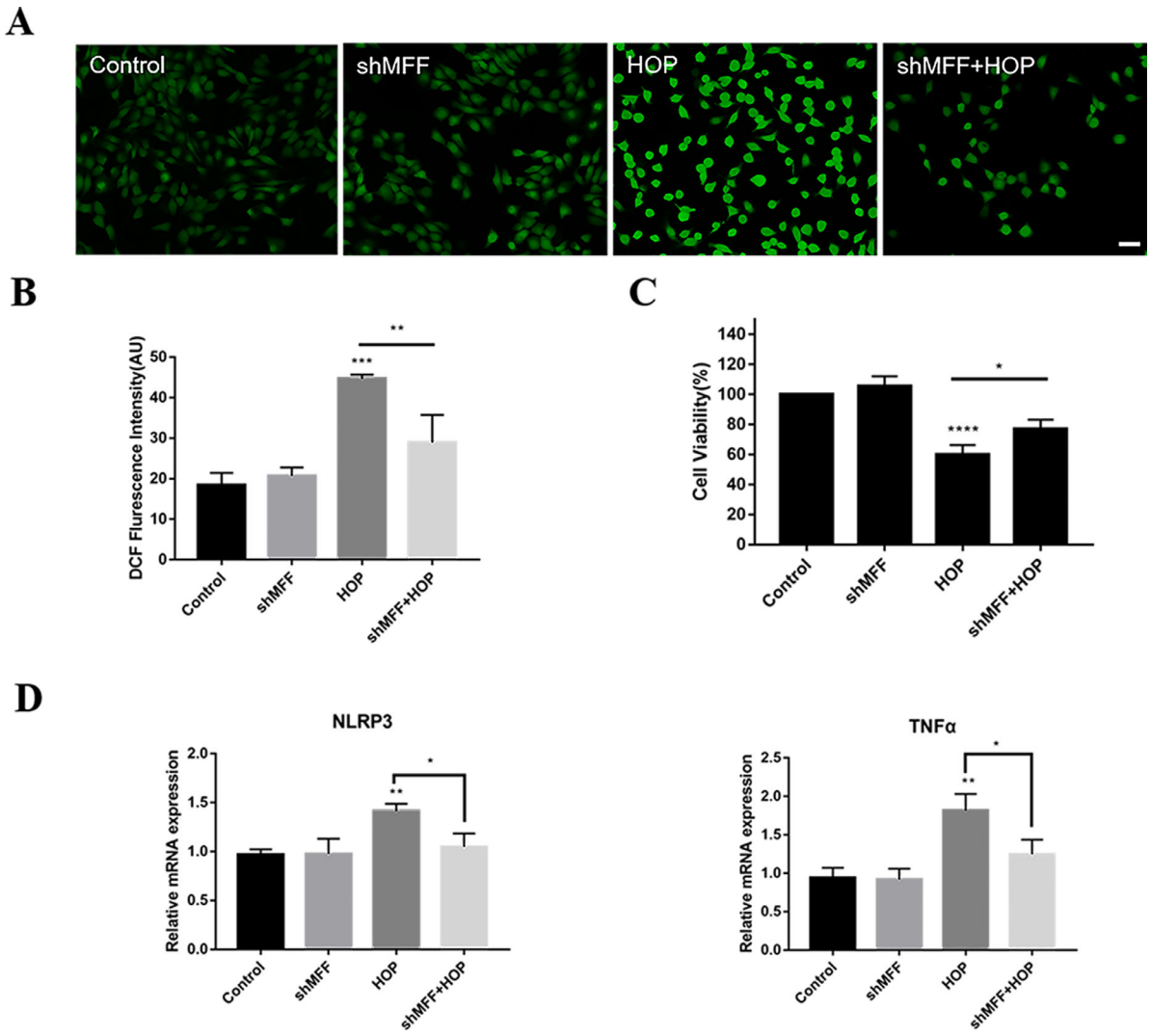

Figure 7. Knockdown of MFF alleviated increased ROS and inflammatory factors under hyperosmolar conditions. HCECs transfected with blank and shRNA of MFF lentiviral vectors were exposed to normal or hyperosmotic medium for 24 hours. (**A**) The results of intracellular ROS in HCECs by H_2DCFDA assay. *Scale bar*: 50 µm. (**B**) Statistical results of the mean fluorescence intensity of intracellular ROS in HCECs. (**C**) Changes to cell viability by CCK-8 assay following MFF knockdown. (**D**) Results of RT-PCR for gene expression of intracellular inflammatory factors NLRP3 and TNF-α. Three independent experiments were conducted, and results are presented as mean + SD. $^{*}P < 0.05$, $^{**}P < 0.01$, $^{***}P < 0.001$, $^{****}P < 0.0001$.

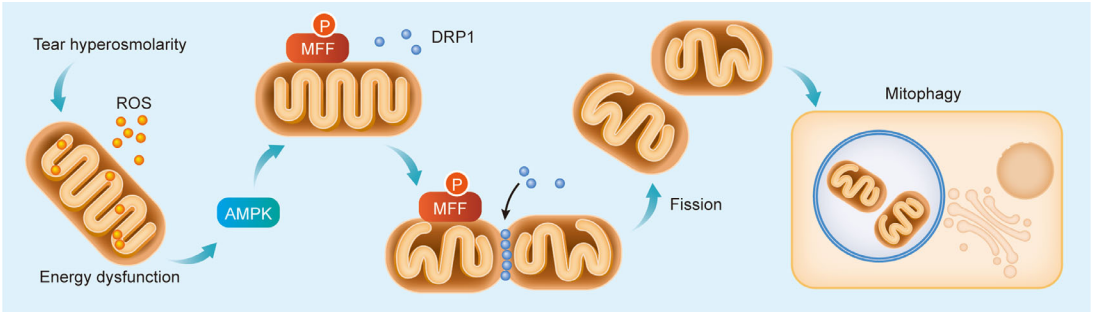

Figure 8. Graphic overview. In dry eye, tear hyperosmolarity triggers mtROS and cell energy dysfunction, possibly activating AMPK/MFF in HCECs. MFF activation recruits cytoplasmic DRP1 to the outer mitochondrial membrane and mediates mitochondrial fission and mitophagy.

autophagy.[19] Our results suggest that the knockdown of MFF reduced ROS release, decreased NLRP3 and TNF-α gene expression, and enhanced the cell viability of HCECs after exposure to HOP. Thus, inhibition of mitochondrial fission

Investigative Ophthalmology & Visual Science

may partially rescue dry eye. Cid-Castro et al.[41] reported that increased ROS in neurons promoted DRP1 activation, leading to increased mitochondrial fission that further increased ROS production, whereas DRP1 knockdown reduced oxidative stress-induced mitochondrial fission.[37] ROS and mitochondrial fission form a vicious cycle that aggravates mitochondrial dysfunction, increases ROS levels, and increases brain damage after stroke.[42] Our study confirmed that increased ROS in HCECs promotes mitochondrial fission. Excitingly, inhibition of mitochondrial fission by MFF inhibition reduced cellular ROS. Collectively, breaking the vicious cycle of ROS and mitochondrial fission may be important in the treatment of dry eye.

We first detected altered mitochondrial morphology in dry eye. Furthermore, we have illustrated that the potential mechanism of mitochondrial fission is the activation of AMPK/MFF sensing cellular energy stress. Nevertheless, the present study did not explore changes to mitochondrial morphology and mitophagy with associated genetic intervention in vivo.

In summary, this study identified abnormally increased mitochondrial fission and mitophagy in HCECs in dry eye. Energy stress induced by HOP led to activation of AMPK/MFF with consequent recruitment of DRP1 to translocate from the cytoplasm to the outer mitochondrial membrane to mediate mitochondrial fission and mitophagy. Importantly, attenuation of mitochondrial fission by MFF inhibition alleviated oxidative stress and inflammation in dry eye. This study presents a novel foundation for future research and treatment of patients with dry eye disease.

Acknowledgments

Supported by research grants from the National Natural Science Foundation of China (81970770 and 82171021 to WC).

Disclosure: **F. Peng**, None; **D. Jiang**, None; **W. Xu**, None; **Y. Sun**, None; **Z. Zha**, None; **X. Tan**, None; **J. Yu**, None; **C. Pan**, None; **Q. Zheng**, None; **W. Chen**, None

References

1. Mizuno Y, Yamada M, Shigeyasu C. Annual direct cost of dry eye in Japan. *Clin Ophthalmol*. 2012;6:755–760.
2. Li M, Gong L, Chapin WJ, Zhu M. Assessment of vision-related quality of life in dry eye patients. *Invest Ophthalmol Vis Sci*. 2012;53:5722–5727.
3. Bron AJ, de Paiva CS, Chauhan SK, et al. Corrigendum to "TFOS DEWS II pathophysiology report" [Ocul. Surf. 15 (3) (2017) 438-510]. *Ocul Surf*. 2019;17:842.
4. Aldrich BT, Schlötzer-Schrehardt U, Skeie JM, et al. Mitochondrial and morphologic alterations in native human corneal endothelial cells associated with diabetes mellitus. *Invest Ophthalmol Vis Sci*. 2017;58:2130–2138.
5. Archer SL. Mitochondrial dynamics–mitochondrial fission and fusion in human diseases. *N Engl J Med*. 2013;369:2236–2251.
6. Anderson S, Bankier AT, Barrell BG, et al. Sequence and organization of the human mitochondrial genome. *Nature*. 1981;290:457–465.
7. De Palma C, Falcone S, Pisoni S, et al. Nitric oxide inhibition of Drp1-mediated mitochondrial fission is critical for myogenic differentiation. *Cell Death Differ*. 2010;17:1684–1696.
8. Molina AJ, Wikstrom JD, Stiles L, et al. Mitochondrial networking protects β-cells from nutrient-induced apoptosis. *Diabetes*. 2009;58:2303–2315.
9. Wang H, Lim PJ, Karbowski M, Monteiro MJ. Effects of overexpression of huntingtin proteins on mitochondrial integrity. *Hum Mol Genet*. 2009;18:737–752.
10. Palikaras K, Lionaki E, Tavernarakis N. Mechanisms of mitophagy in cellular homeostasis, physiology and pathology. *Nat Cell Biol*. 2018;20:1013–1022.
11. Iorio R, Celenza G, Petricca S. Mitophagy: molecular mechanisms, new concepts on Parkin activation and the emerging role of AMPK/ULK1 axis. *Cells*. 2021;11:30.
12. Haq S, Grondin J, Banskota S, Khan WI. Autophagy: roles in intestinal mucosal homeostasis and inflammation. *J Biomed Sci*. 2019;26:19.
13. Pal R, Palmieri M, Loehr JA, et al. Src-dependent impairment of autophagy by oxidative stress in a mouse model of Duchenne muscular dystrophy. *Nat Commun*. 2014;5:4425.
14. Wang B, Peng L, Ouyang H, et al. Induction of DDIT4 impairs autophagy through oxidative stress in dry eye. *Invest Ophthalmol Vis Sci*. 2019;60:2836–2847.
15. Liu Z, Chen D, Chen X, et al. Trehalose induces autophagy against inflammation by activating TFEB signaling pathway in human corneal epithelial cells exposed to hyperosmotic stress. *Invest Ophthalmol Vis Sci*. 2020;61:26.
16. Tilokani L, Nagashima S, Paupe V, Prudent J. Mitochondrial dynamics: overview of molecular mechanisms. *Essays Biochem*. 2018;62:341–360.
17. Eisner V, Picard M, Hajnóczky G. Mitochondrial dynamics in adaptive and maladaptive cellular stress responses. *Nat Cell Biol*. 2018;20:755–765.
18. Toyama EQ, Herzig S, Courchet J, et al. Metabolism. AMP-activated protein kinase mediates mitochondrial fission in response to energy stress. *Science*. 2016;351:275–281.
19. Zheng Q, Zhao Y, Guo J, et al. Iron overload promotes mitochondrial fragmentation in mesenchymal stromal cells from myelodysplastic syndrome patients through activation of the AMPK/MFF/Drp1 pathway. *Cell Death Dis*. 2018;9:515.
20. Ducommun S, Deak M, Sumpton D, et al. Motif affinity and mass spectrometry proteomic approach for the discovery of cellular AMPK targets: identification of mitochondrial fission factor as a new AMPK substrate. *Cell Signal*. 2015;27:978–988.
21. Mihaylova MM, Shaw RJ. The AMPK signalling pathway coordinates cell growth, autophagy and metabolism. *Nat Cell Biol*. 2011;13:1016–1023.
22. Prakash YS, Pabelick CM, Sieck GC. Mitochondrial dysfunction in airway disease. *Chest*. 2017;152:618–626.
23. Fridovich I. Superoxide radical and superoxide dismutases. *Annu Rev Biochem*. 1995;64:97–112.
24. Li Y, Huang TT, Carlson EJ, et al. Dilated cardiomyopathy and neonatal lethality in mutant mice lacking manganese superoxide dismutase. *Nat Genet*. 1995;11:376–381.
25. Zheng Q, Tan Q, Ren Y, et al. Hyperosmotic stress-induced TRPM2 channel activation stimulates NLRP3 inflammasome activity in primary human corneal epithelial cells. *Invest Ophthalmol Vis Sci*. 2018;59:3259–3268.
26. Zheng Q, Ren Y, Reinach PS, et al. Reactive oxygen species activated NLRP3 inflammasomes initiate inflammation in hyperosmolarity stressed human corneal epithelial cells and environment-induced dry eye patients. *Exp Eye Res*. 2015;134:133–140.
27. Dursun D, Wang M, Monroy D, et al. A mouse model of keratoconjunctivitis sicca. *Invest Ophthalmol Vis Sci*. 2002;43:632–638.
28. Zheng Q, Ren Y, Reinach PS, et al. Reactive oxygen species activated NLRP3 inflammasomes prime environment-induced murine dry eye. *Exp Eye Res*. 2014;125:1–8.

29. Toyama EQ, Herzig S, Courchet J, et al. Metabolism. AMP-activated protein kinase mediates mitochondrial fission in response to energy stress. *Science*. 2016;351:275–281.
30. Kahn BB, Alquier T, Carling D, Hardie DG. AMP-activated protein kinase: ancient energy gauge provides clues to modern understanding of metabolism. *Cell Metab*. 2005;1:15–25.
31. Vafai SB, Mootha VK. Mitochondrial disorders as windows into an ancient organelle. *Nature*. 2012;491:374–383.
32. Liesa M, Shirihai OS. Mitochondrial dynamics in the regulation of nutrient utilization and energy expenditure. *Cell Metab*. 2013;17:491–506.
33. Tezze C, Romanello V, Desbats MA, et al. Age-associated loss of OPA1 in muscle impacts muscle mass, metabolic homeostasis, systemic inflammation, and epithelial senescence. *Cell Metab*. 2017;25:1374–1389.e6.
34. Parra V, Verdejo HE, Iglewski M, et al. Insulin stimulates mitochondrial fusion and function in cardiomyocytes via the Akt-mTOR-NFκB-Opa-1 signaling pathway. *Diabetes*. 2014;63:75–88.
35. Cheng CT, Kuo CY, Ouyang C, et al. Metabolic stress-induced phosphorylation of KAP1 Ser473 blocks mitochondrial fusion in breast cancer cells. *Cancer Res*. 2016;76:5006–5018.
36. Yu T, Robotham JL, Yoon Y. Increased production of reactive oxygen species in hyperglycemic conditions requires dynamic change of mitochondrial morphology. *Proc Natl Acad Sci USA*. 2006;103:2653–2658.
37. Youle RJ, van der Bliek AM. Mitochondrial fission, fusion, and stress. *Science*. 2012;337:1062–1065.
38. Chan DC. Fusion and fission: interlinked processes critical for mitochondrial health. *Annu Rev Genet*. 2012;46:265–287.
39. Lu YT, Li LZ, Yang YL, et al. Succinate induces aberrant mitochondrial fission in cardiomyocytes through GPR91 signaling. *Cell Death Dis*. 2018;9:672.
40. Pascucci B, Spadaro F, Pietraforte D, et al. DRP1 inhibition rescues mitochondrial integrity and excessive apoptosis in CS-A disease cell models. *Int J Mol Sci*. 2021;22:7123.
41. Cid-Castro C, Hernández-Espinosa DR, Morán J. ROS as regulators of mitochondrial dynamics in neurons. *Cell Mol Neurobiol*. 2018;38:995–1007.
42. Hwang JA, Shin N, Shin HJ, et al. Protective effects of ShcA protein silencing for photothrombotic cerebral infarction. *Transl Stroke Res*. 2021;12:866–878.